Recycling of aborted ribosomal 50S subunit-nascent chain-tRNA complexes by the heat shock protein Hsp15

Jiang, L.; Schaffitzel, C.; Bingel-Erlenmeyer, R.; Ban, N.; Korber, K.P.; Geus, D.C. de; ... ; Abrahams, J.P.

doi:10.1016/j.jmb.2008.10.079 J. Mol. Biol. (2009) 386, 1357–1367

JMB

Available online at www.sciencedirect.com

ScienceDirect

ELSEVIER

Recycling of Aborted Ribosomal 50S Subunit-Nascent Chain-tRNA Complexes by the Heat Shock Protein Hsp15

Linhua Jiang[1], Christiane Schaffitzel[2], Rouven Bingel-Erlenmeyer[2], Nenad Ban[2], Philipp Korber[3], Roman I. Koning[4], Daniël C. de Geus[1], Jasper R. Plaisier[1] and Jan Pieter Abrahams[1]*

[1]*Department of Biophysical Structural Chemistry, Leiden Institute of Chemistry, Leiden University, Einsteinweg 55, 2333 CC Leiden, The Netherlands*

[2]*Institute for Molecular Biology and Biophysics, ETH Zurich, HPK Building, Schafmattstr. 20, 8093 Zurich, Switzerland*

[3]*Adolf Butenandt Institut, Molekularbiologie, LMU Munich, Schillerstr. 44, 80336 Munich, Germany*

[4]*Electron Microscopy Section, Department of Molecular Cell Biology, Leiden University Medical Center, P.O. Box 9600, 2300 RC, Leiden, The Netherlands*

Received 9 June 2008; received in revised form 19 September 2008; accepted 26 October 2008
Available online 5 November 2008

Edited by J. Doudna

When heat shock prematurely dissociates a translating bacterial ribosome, its 50S subunit is prevented from reinitiating protein synthesis by tRNA covalently linked to the unfinished protein chain that remains threaded through the exit tunnel. Hsp15, a highly upregulated bacterial heat shock protein, reactivates such dead-end complexes. Here, we show with cryo-electron microscopy reconstructions and functional assays that Hsp15 translocates the tRNA moiety from the A site to the P site of stalled 50S subunits. By stabilizing the tRNA in the P site, Hsp15 indirectly frees up the A site, allowing a release factor to land there and cleave off the tRNA. Such a release factor must be stop codon independent, suggesting a possible role for a poorly characterized class of putative release factors that are upregulated by cellular stress, lack a codon recognition domain and are conserved in eukaryotes.

Keywords: Hsp15; ribosome; tRNA; heat shock; cryo-EM

Introduction

Heat shock upregulates many proteins that function as chaperones or proteases. It also increases the transcription of the small heat shock protein Hsp15, which is an RNA/DNA binding protein. It targets aborted ribosomal 50S subunits rather than misfolded proteins.[1] Its ~50-fold transcriptional increase is even higher than the upshift in expression of such well-characterized heat shock proteins as GroEL/ES, DnaK and ClpA, indicating the high relevance of Hsp15 for adapting to thermal stress.[2]

Translating ribosomes can dissociate prematurely upon heat shock, resulting in 50S subunits that carry tRNA covalently attached to the nascent chain (nc-tRNA) of an incomplete protein that is

*Corresponding author. E-mail address: abrahams@chem.leidenuniv.nl.

Abbreviations used: nc-tRNA, nascent chain-tRNA; EM, electron microscopy; FSC, Fourier shell correlation.

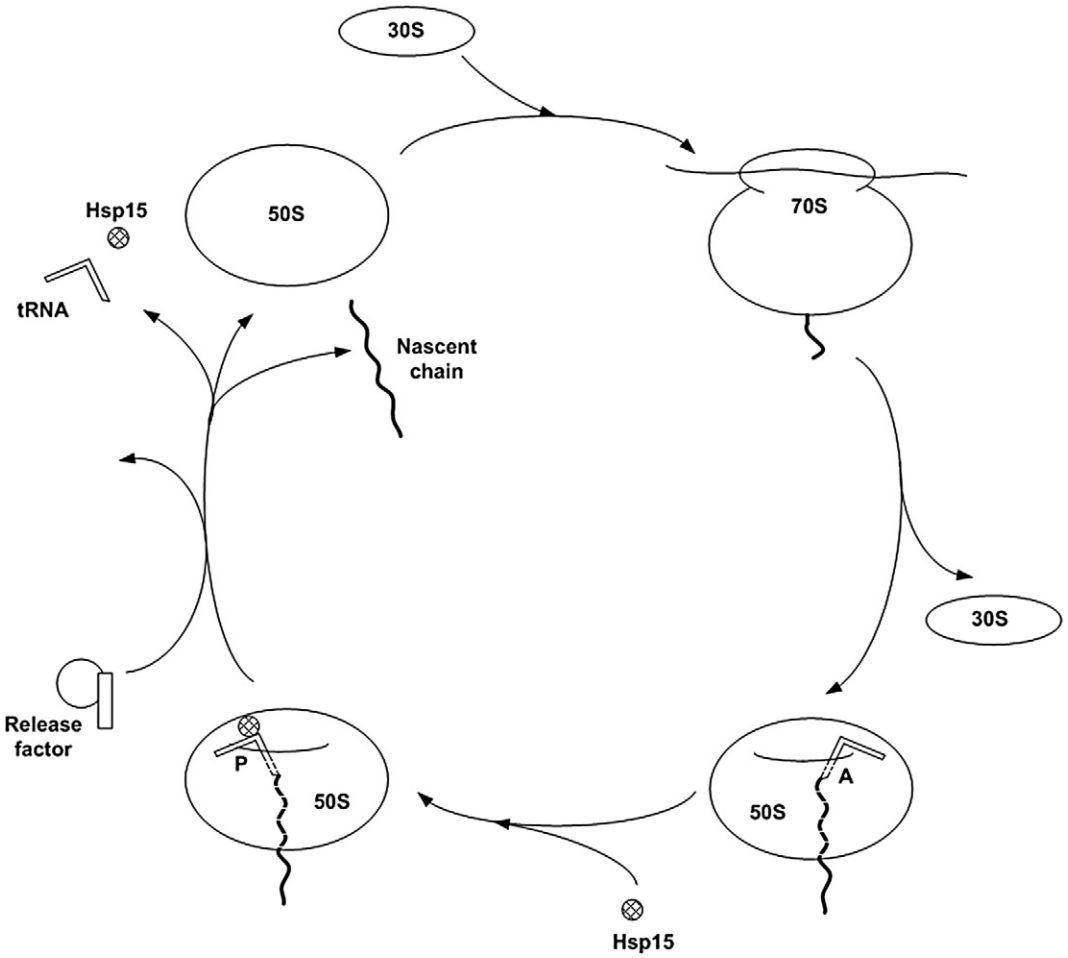

Fig. 1. Rescue cycle of the stalled ribosomal 50S subunit. Heat shock can erroneously dissociate a translating ribosome into a 30S subunit and a blocked 50S subunit carrying a tRNA linked to the unfinished nascent chain (lower right). Here, we show that in these stalled 50S•nc-tRNA complexes, the tRNA is located at the A site (bottom right) and that the small heat shock protein Hsp15 translocates the tRNA to the P site (bottom left), where it can be liberated by a release factor (top left).

threaded through the 50S exit tunnel (Fig. 1)†. These 50S•nc-tRNA subunits cannot reinitiate protein synthesis, and their accumulation would constitute a problem for the cell. In the intact 70S ribosome, the tRNA is released from the nascent chain by a release factor, which binds in the vacant A site to cleave the peptidyl ester bond. All well-characterized release factors are stop codon dependent,[3–5] yet the release factor that recycles blocked 50S subunits must be stop codon independent as there is no stop codon in the dissociated 50S subunit.

Such blocked 50S subunits are rescued by Hsp15, which specifically binds blocked 50S•nc-tRNA ribosomal subunits with high affinity (K_d<5 nM), while its affinity for empty, functional 50S subunits is significantly lower.[6] It was established that Hsp15 is not a release factor, since the 50S•nc-tRNA•Hsp15 is stable and the tRNA moiety is not released.[7] It remains unclear how Hsp15 discriminates between active and aberrantly terminated 50S subunits and how it contributes to recycling blocked, nonfunctional 50S•nc-tRNA complexes.

To answer these questions, we determined the structure of the complex of the 50S•nc-tRNA subunit in the absence and in the presence of Hsp15 by cryo-electron microscopy (EM) and single-particle analysis to resolutions of 14 and 10 Å, respectively. The resolution was sufficiently high to fit atomic models of the individual components (50S, tRNA and Hsp15) into the EM density maps. We confirmed our results with puromycin nascent chain release assays.

Results

Generation of stable 50S•nc-tRNA complexes

Stable, homogenous 70S•nc-tRNA complexes were generated by *in vitro* transcription and *in vitro*

† Presumably, tRNA attached to a short peptide would still dissociate, hence our use of the term "nc–tRNA" throughout this article to distinguish it from tRNA attached to very short peptides.

translation using the plasmid pUC19Strep3FtsQ-SecM with an N-terminal triple Strep tag for affinity purification.[7] The FtsQ sequence and the 17-aa-long SecM translational arrest motif were C-terminally fused to the affinity tag to span the ribosomal exit tunnel. The SecM peptide interacts tightly with the ribosomal tunnel[8] and thereby significantly stabilizes the 70S•nc-tRNA complexes, without the need for using chloramphenicol antibiotic. After *in vitro* translation, the translating ribosomes were loaded onto a sucrose gradient with a low concentration of magnesium ions, causing dissociation of the 70S•nc-tRNA complexes into 50S•nc-tRNA and 30S (Fig. 2a) complexes. The 50S•nc-tRNA complexes were further purified and separated from empty 50S using a StrepTactin Sepharose column and finally pelleted by ultracentrifugation. The complex with Hsp15 was reconstituted by adding a 20-fold molar excess of Hsp15.

Binding assays confirmed that Hsp15 binds neither 70S ribosomes nor empty 50S subunits under the assay conditions (Fig. 2b). However, a low level of binding of Hsp15 to empty 50S subunits was observed when the sucrose cushion was omitted from the sedimentation assay (data not shown). This is in agreement with the previously described nonspecific nucleic acid binding activity of Hsp15.[1] Hsp15 only had a high affinity for 50S subunits when they contained nc-tRNA. Also, Hsp15 had to be present in a 1:10 molar ratio (Fig. 2b).

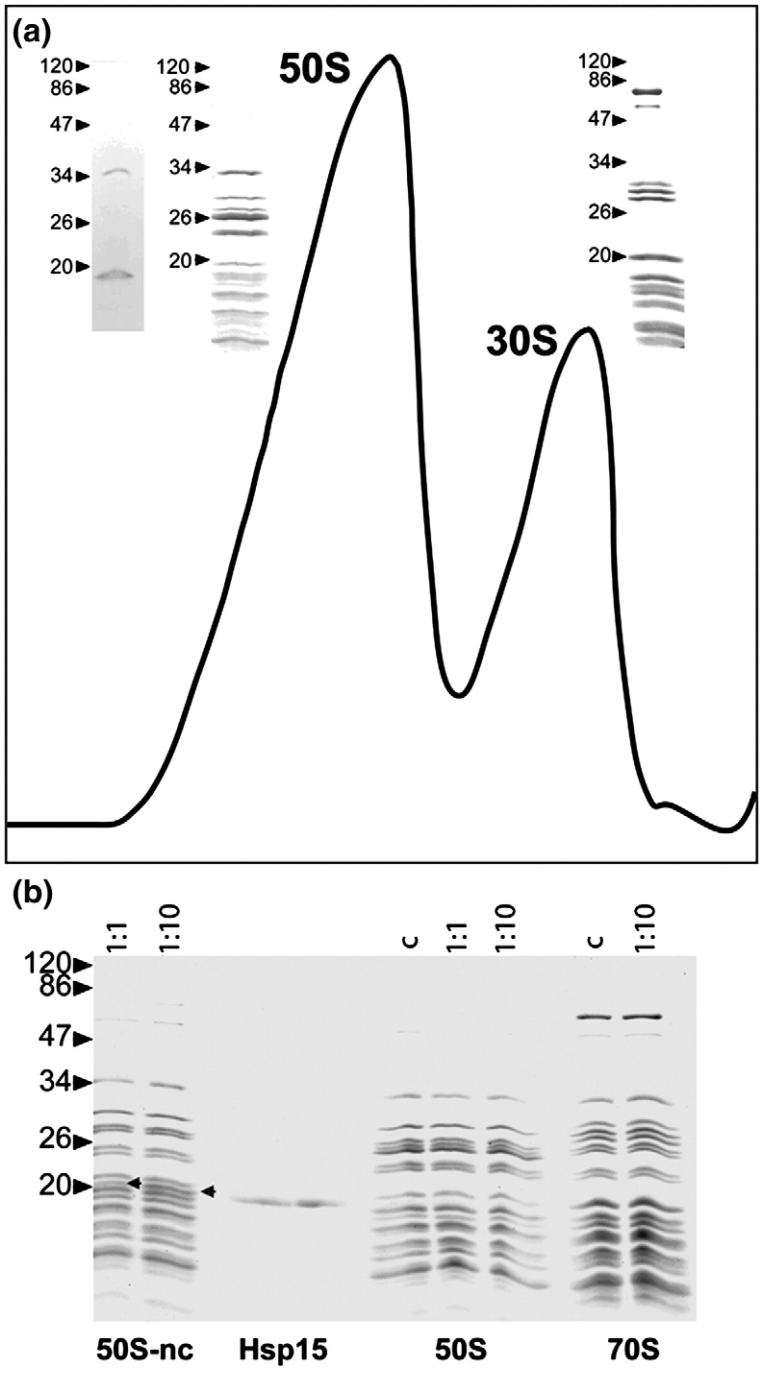

Fig. 2. (a) Preparation of 50S•nc-tRNA complexes (50S•nc/50S•nc-tRNA). Sucrose gradient profile of an *in vitro* translation reaction in the presence of 0.3 mM $Mg(OAc)_2$. The two peaks (50S and 30S) were analyzed on a Coomassie-stained SDS gel. The presence of the nascent chain in the 50S is shown by Western blotting (left side) using StrepTactin–alkaline phosphatase conjugate. The upper band at ~34 kDa corresponds to nc-tRNA; the lower band, to the nascent peptide alone. (b) Binding assay of Hsp15. Binding of purified Hsp15 to 50S•nc, that to 50S and that to 70S were analyzed by ribosomal pelleting through a sucrose cushion. As a control (indicated with *c*), 50S and 70S were loaded alone. Hsp15 did not migrate through the sucrose cushion (not shown). Hsp15 was added in 1:1 and 1:10 molar ratios. Hsp15 was found only in the pellet of 50S•nc as indicated with arrows in lanes 1 and 2; in the 1:1 molar ratio, somewhat less Hsp15 was recovered. As a positive control, 100 ng of Hsp15 was loaded onto the SDS gel.

Structure of the 50S·nc-tRNA complex

In order to identify the position of Hsp15 in the ribosomal complex, we first determined the structure of the 50S subunit-containing nc-tRNA in the absence of Hsp15 by single-particle cryo-EM. In two separate reconstructions, we used (i) the cryo-EM reconstruction of the empty 50S subunit (see Supplementary Data) and (ii) the model of the 50S•nc-tRNA complex that did contain Hsp15 (see below) as starting models. The two reconstructions converged to a similar structure of about 14-Å resolution [Fourier shell correlation (FSC) criterion = 50%], the main features of which were confirmed in a comparison with structures reported earlier. Only the L7/L12 stalk of the 50S subunit was not fully visible in our reconstruction, but this region is known to be flexible and conformationally heterogeneous in isolated large ribosomal subunits.[9] More importantly, the structure revealed clear additional density located at the A site (Fig. 3a), corresponding to the tRNA covalently attached to the nascent polypeptide that is extending through the ribosomal exit tunnel.

Structure of the 50S·nc-tRNA·Hsp15 complex

The reconstruction of the 50S·nc-tRNA·Hsp15 complex yielded a resolution of 10 Å based on the FSC (Fig. S2). Clear additional density for tRNA is visible in the P site (Fig. 3b). Supervised classification, aimed at sorting out and removing any empty or deviant 50S particles from the reconstruction, confirmed the biochemical purity of the sample and indicated that the P site was virtually fully occupied with tRNA. The extra density in the P site matched the atomic model of $tRNA^{Phe}$ at contouring levels suggested by other parts of the structure, which indicated that the tRNA is very well ordered in the 50S·nc-tRNA·Hsp15 complex. Its anticodon stem was rotated about 20° about its acceptor stem toward ribosomal protein L1, compared with its location in the crystal structure of the *Thermus thermophilus* 70S ribosome complexed with mRNA and two tRNAs[10] (Fig. 4). Since the angle between the aminoacyl acceptor stem and the anticodon stem can vary in tRNAs,[11] we refined the angle between these stems. This resulted in a small increase (~15°), compared with the crystal structure of $tRNA^{Phe}$, thus somewhat opening up the canonical L-shaped conformation of the tRNA.

In order to locate Hsp15, we first fitted the high-resolution crystal structure of the *Escherichia coli* 50S subunit from the 70S complex[12] into our density using multiple rigid-body fitting for the ribosomal RNA and proteins. Proteins L1, L11, L7 and L12 could not be fitted well into our density map. Most of these proteins are known to be flexible and therefore were not included in the final model. We identified well-ordered extra density close to the P-site nc-tRNA. This extra density was located between the base of the central protuberance of 50S and the elbow region of the nc-tRNA. No known component of the 50S subunit could explain the extra density, and neither could the tRNA be docked into it without gross distortions and vacating other densities. A small part of the extra density did overlap with the highly disordered S72–R79 loop of protein L5, but the density of this loop was not visible in the reconstruction of the 50S•nc-tRNA complex, and it has a mean temperature factor well above 100 $Å^2$ in the crystal structure of the complete 70S complex.[12] We concluded that this fragment of L5 could not explain the additional density. At increased contour levels, corresponding to highly ordered parts of the structure, a tube-like feature in the extra density was visible. Assuming this feature corresponded to the C-terminal α-helix of Hsp15, we docked the atomic structure of monomeric Hsp15[13] into this extra density and refined its position using our program

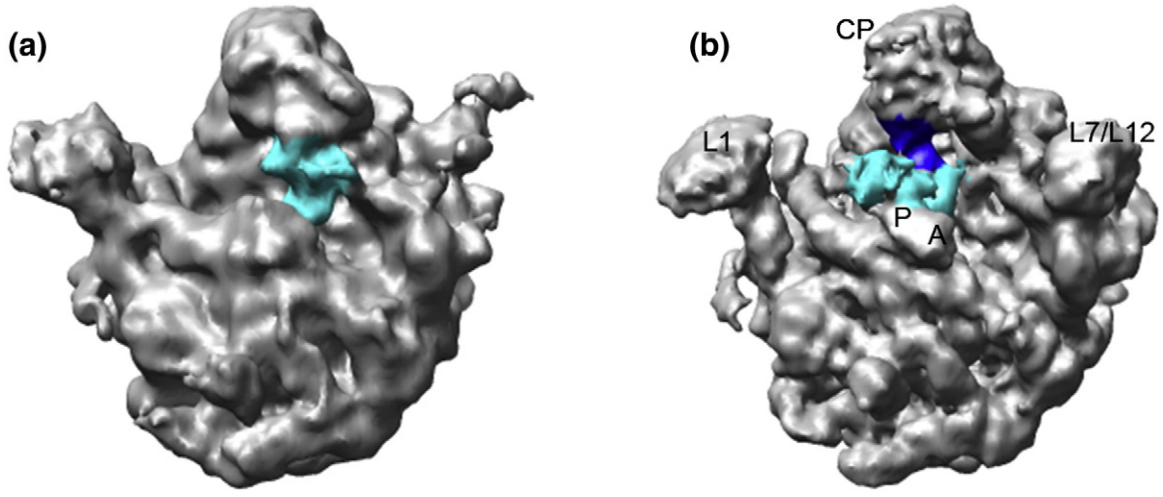

Fig. 3. Reconstructions of (a) the 50S•nc-tRNA complex (the density of tRNA is in cyan, 14-Å resolution) and (b) the 50S•nc-tRNA•Hsp15 complex (the density of tRNA is in cyan and that of Hsp15 is in blue, 10-Å resolution). The central protuberance (CP), the L1 and L7/L12 domains and the P and A sites are indicated.

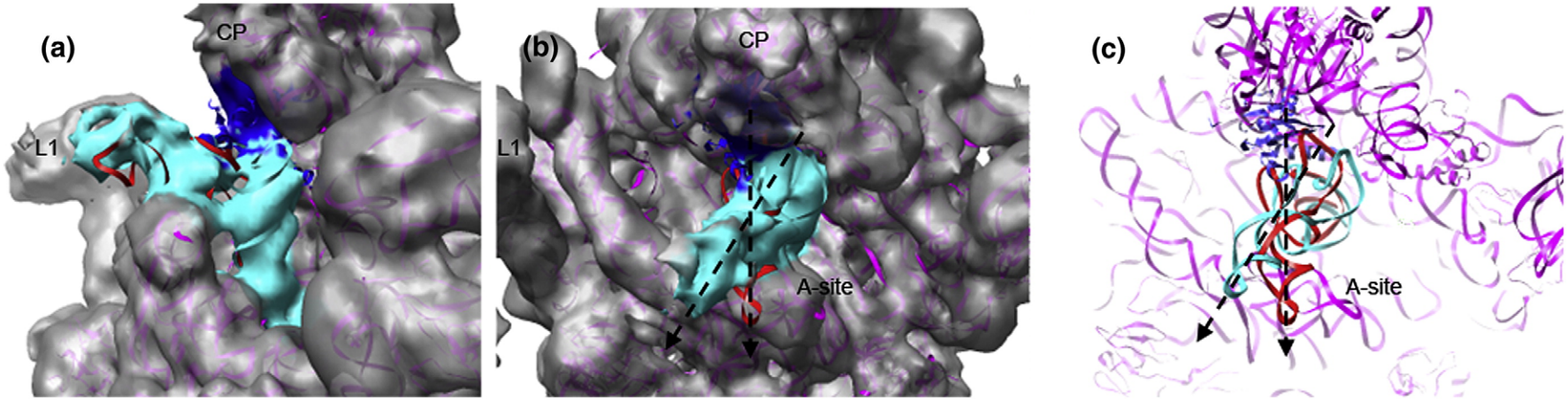

Fig. 4. Side (a) and top (b) views of the 50S subunit and tRNA of the crystal structure of the *T. thermophilus* 70S·tRNA complex docked into the density of the 50S•nc-tRNA·Hsp15 complex. The density corresponding to 50S is depicted in gray, tRNA density is in cyan and Hsp15 density is in blue. (c) Same as (b) but without the density. The high-resolution structure of the 50S *T. thermophilus* subunit and its cognate tRNA[10] are shown as a purple and red ribbons, respectively. The position of the blue density indicates a 20° rotation of the tRNA in the 50S•nc-tRNA·Hsp15 complex about its aminoacyl acceptor stem compared with the position of the tRNA in the 70S crystal structure. The main axes of the tRNAs are indicated by arrows. The central protuberance (CP), the L1 domain and the A site are indicated.

LOCALFIT (to be described elsewhere). The resulting atomic model is shown in Fig. 5.

Hsp15 is known to have an αL RNA binding motif (also known as the S4 RNA binding motif), which it shares with ribosomal protein S4 and threonyl-tRNA synthetase, among others.[13] The structural details of the interaction of S4 with its cognate helixes H16-18 of 16S RNA are known, and we investigated whether S4 and Hsp15 interact with their target RNA binding sites in a similar fashion. For this purpose, we superimposed the αL RNA binding motifs of both proteins and applied the same geometric operator to their cognate RNAs. This comparison indicated that the αL RNA binding domains of Hsp15 and S4 interacted in the same fashion with their cognate RNA targets (Fig. 6).

The long C-terminal α-helix opposite the RNA binding motif of Hsp15 and the ultimate 23 C-terminal residues (which are disordered in the crystal structure) carry a substantial number of positive charges. This C-terminal α-helix contacted the D/T loops of the nc-tRNA, and, although the C-terminus, which is disordered in the crystal structure, could not be visualized in our EM density, there is sufficient space for its positive charges to interact with the nc-tRNA and/or proximal regions of 23S ribosomal RNA.

Functional assay of Hsp15-induced tRNA translocation

The P site-specific antibiotic puromycin is a functional equivalent of a stop codon-independent release factor. Mimicking the 3′ end of aminoacyl tRNA at the A site, it binds at the A site and cleaves off P-site tRNA from the nascent chain. It is used in functional assays to distinguish P-site tRNA from A-site tRNA and establish A-site occupancy. It was established that puromycin abolishes binding of Hsp15 to 50S•nc-tRNA complexes in cell extracts.[6] Presumably, puromycin released the tRNA from the 50S subunit and the resulting empty 50S subunits

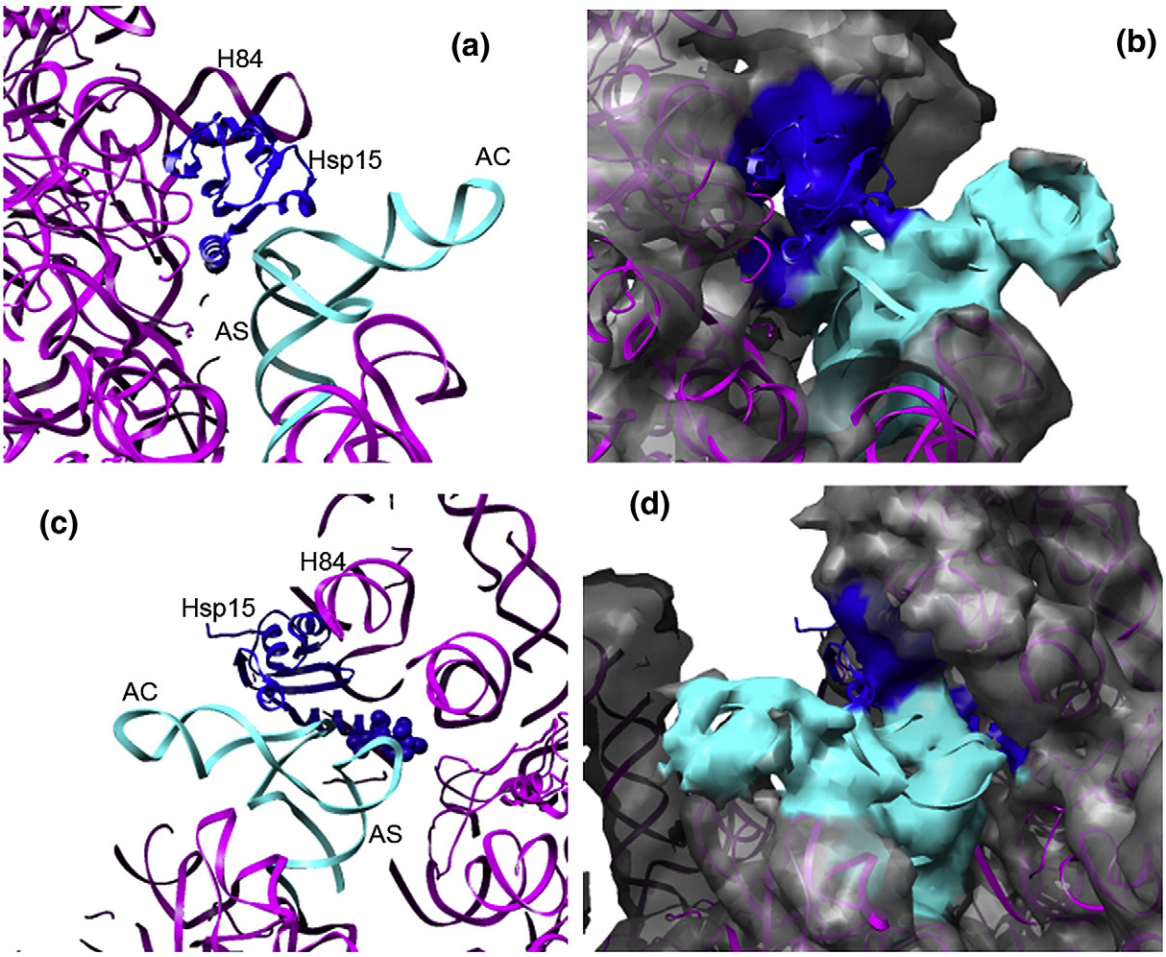

Fig. 5. Hsp15 attaches to the H84 helix of the 23S ribosomal RNA and interacts with the D/T loops of the tRNA. (a) View from the left with respect to the standard orientation of the 50S subunit (see Fig. 2). The 50S subunit is depicted in magenta, and the tRNA is in cyan. (b) Same as (a), including the 50S•nc-tRNA complex density; density covering Hsp15 is shown in blue, that covering tRNA is shown in cyan and that covering 50S is shown in gray. (c) Interaction of the tail of Hsp15 and tRNA; right side view, the C-terminal positively charged α-helix of Hsp15 is shown as spheres. (d) Same as (c), showing density contoured at a level predicted by the molecular weight of the 50S•nc-tRNA•Hsp15 complex. Helix 84 of 23S RNA (H24), the anticodon stem (AC) and the aminoacyl acceptor stem (AS) of the P-site nc-tRNA are indicated.

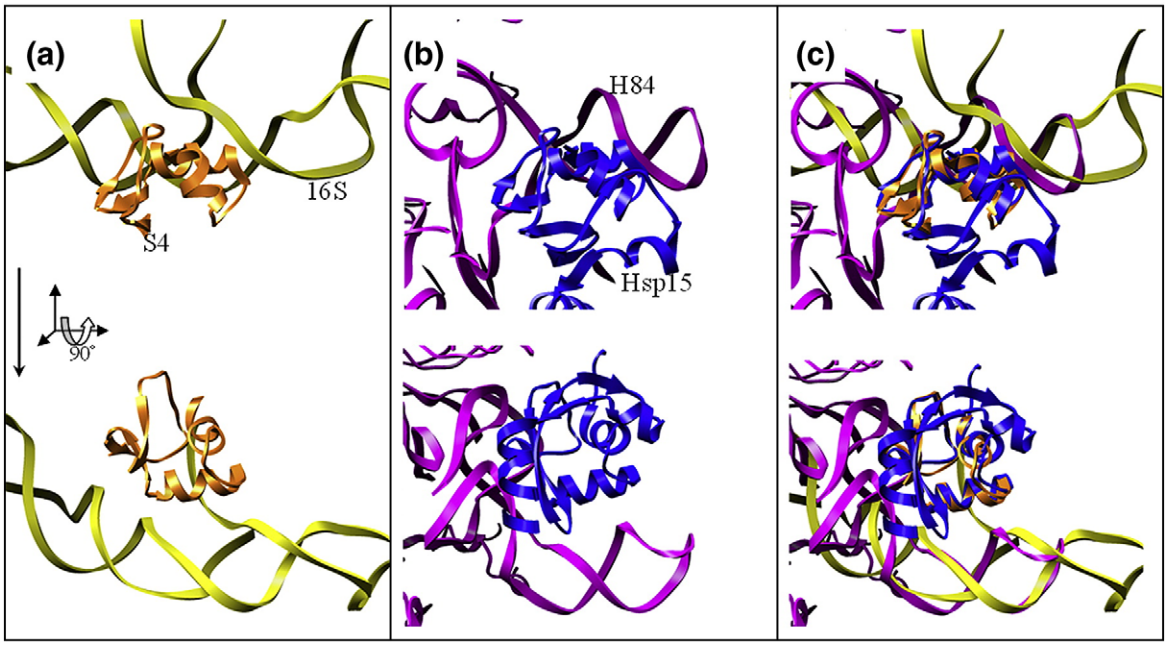

Fig. 6. Comparison of the RNA binding modes of S4 and Hsp15. (a) Top and side views (below) of S4 interacting through its αL binding motif with its cognate 16S RNA fragment. (b) Top and side views of Hsp15 interacting through its αL binding motif with helix84 of 23S ribosomal RNA. (c) Superimposition of (a) and (b). The RNA binding motifs of Hsp15 (blue) and S4 (orange) were superimposed; the fragment of 16S RNA that is recognized by S4 is shown in yellow and fits well with 23S RNA, indicating that Hsp15 and S4 bind in a similar fashion to dsRNA.

would no longer have a high affinity for Hsp15. This observation already indicated that the tRNA must reside in the P site in the 50S•nc-tRNA•Hsp15 complex in cell extracts. Here, we show that no additional factor was involved: also, in highly purified 50S•nc-tRNA•Hsp15 samples, puromycin was able to cleave off the nascent chain (Fig. 7).

N-acetylated Phe-$tRNA_{Phe}$ is an nc-tRNA homolog that can freely diffuse into and out of the P site of 50S subunits, where it can react with A site-bound puromycin. This reaction proceeds optimally at 100 mM Mg^{2+} in isolated 50S subunits but is slower at lower Mg^{2+} concentrations.[14] However, for the 50S•nc-tRNA•Hsp15 complex, we found the opposite effect: raising the Mg^{2+} concentration *reduced* the puromycin reactivity.

The cryo-EM structure provided a straightforward explanation for this observation. At 100 mM Mg^{2+}, Hsp15 dissociates more easily from 50S•nc-tRNA complexes.[6] If Hsp15 is essential for stabilizing the tRNA moiety in the P site, as suggested by the structures, then its dissociation from the 50S·nc-tRNA·Hsp15 complex should result in a relocation of the tRNA to the A site, where it cannot be cleaved by puromycin.

Discussion

Translational reactivation of a heat shock-aborted 50S•nc-tRNA complex requires removal of the nc-tRNA by severing of the aminoacyl ester bond between these moieties. In the cell, this hydrolysis requires the tRNA to be located in the P site and a release factor to bind at the vacant A site. In the absence of Hsp15, the tRNA moiety of nc-tRNA, although being somewhat disordered, was clearly located in the A site (Fig. 3a). The A-site location of the tRNA moiety was further corroborated by a puromycin assay (Fig. 7). At first sight, this is a surprising result, as in the complete 70S ribosome, peptidyl-tRNA has a preference for the P site. However, in the 70S complex, peptidyl-tRNA is stabilized at the P site by extensive contacts with the mRNA, 16S RNA and protein residues of the 30S subunit (e.g., Ref. 15), and these interactions are obviously absent in the 50S•nc-tRNA complex. On the other hand, the A-site location of the tRNA is stabilized by additional interactions with residues of the 50S subunit that lie outside the peptidyl transfer center (e.g., helix 38 of the 'A-site finger').[16] Apparently, in the absence of the 30S subunit, these interactions are strong enough to direct the tRNA moiety in the 50S·nc-tRNA complex to the A site. Our observation explains why the 50S•nc-tRNA complex cannot be recycled: a tRNA moiety in the A site prevents release factors from binding and severing the aminoacyl ester bond between the tRNA and the nascent chain.

Hsp15 located the tRNA in the P site by bridging it to helix 84 of the central protuberance of the 50S subunit, the αL RNA binding motif of Hsp15 bound to helix 84, while its positively charged C-terminal tail bound to the D/T loops of the nc-tRNA. Locked in the P site, the CCA end of the nc-tRNA is optimally positioned in the peptidyl transferase center for hydrolytic attack of its aminoacyl ester bond by a release factor. The translocation of the tRNA to

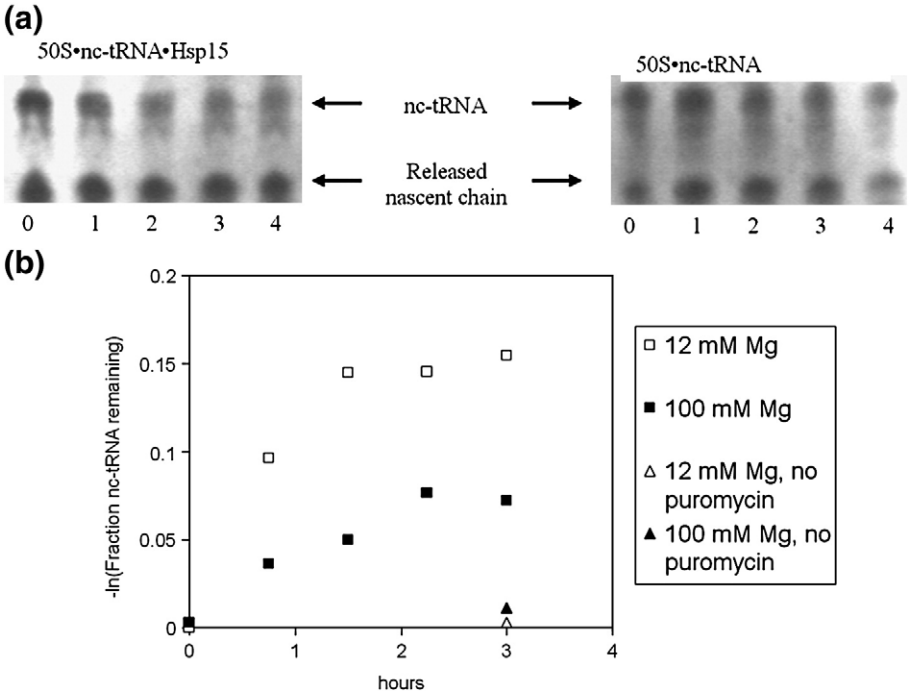

Fig. 7. (a) Puromycin reaction of 50S•nc-tRNA•Hsp15 at 37 °C in 12 mM (left) and 100 mM Mg^{2+} (right). Controls without puromycin do not show any cleavage of the ester bond between tRNA and nascent chain, even after 3 h of incubation. At the outset of the reaction, there is already a substantial amount of released nascent chain present (lower band). (b) The negative natural logarithm of the remaining nc-tRNA was plotted against the incubation time. In a first-order reaction, this is expected to be a straight line, which we indeed observed for 2–3 h after initiating the reaction. The data shown in (a) are plotted. The puromycin-induced cleavage of nc-tRNA was determined by measuring the increase of the intensity of the band corresponding to the released nascent chain as a fraction of the total intensity corresponding to the nascent chain (whether bound to tRNA or not). The higher reactivity at 12 mM Mg^{2+} can be explained by the fixation of tRNA at the P site by Hsp15 at this Mg concentration. The experiments were performed in duplicate.

the P site in the Hsp15-containing complex is in full agreement with the puromycin assay (Fig. 7) and with puromycin sensitivity of dissociated translating ribosomes in cell lysates.[6] Translocation of the nc-tRNA from the A site to the P site would allow a release factor to bind in the A site. In the 70S ribosome, this translocation requires energy: EF-G hydrolyzes GTP in the process. Our results indicate that in the absence of interactions with the 30S subunit, the binding energy of the Hsp15 to the 50S·nc-tRNA complex is sufficient to induce translocation.

Our data also explain why Hsp15 has a reduced affinity for translationally active 50S subunits devoid of nc-tRNA: here, the interaction between the C-terminus of Hsp15 and the P-site tRNA is missing. Furthermore, our data indicate why Hsp15 does not have a marked affinity for translating 70S ribosomes: the presence of the 30S subunit partially blocks access of Hsp15 to its binding site on the 50S subunit, and the conformation of the tRNA interacting simultaneously with the peptidyl transferase center on the 50S subunit and the decoding center on 30S subunit would not allow it to rotate into the position necessary for Hsp15 binding as observed in the EM reconstruction of the 50S•nc-tRNA•Hsp15 complex (Fig. 4c).

Which release factor cleaves the aminoacyl ester bond between the tRNA and the nascent chain in the 50S•nc-tRNA•Hsp15 complex? All well-characterized release factors interact with translating ribosomes and mimic a tRNA molecule. They all have a stop codon-recognizing domain at one end and a GGQ peptidyl hydrolase domain at the other, which interacts with the peptidyl transferase center of the ribosome.[3–5,17] In the blocked 50S•nc-tRNA•Hsp15 complex, there is no stop codon. The putative 15-kDa, 140-aa protein with unassigned function encoded by the *yaeJ* gene in *E. coli* is a likely candidate to serve as a release factor for 50S·nc-tRNA·Hsp15 complexes. In *E. coli*, *yaeJ* is transcribed immediately ahead of *cutF/nplE*, a factor involved in the extracytoplasmic stress response; both apparently belong to the same stress-induced operon.[18] YaeJ contains the conserved GGQ peptidyl hydrolase domain but lacks a stop codon-recognizing domain. Due to the presence of the GGQ motif, YaeJ is placed in the same cluster of orthologous groups as the release factors RF1 and RF2.[17] Thus, YaeJ could bind to the A site of the 50S·nc-tRNA·Hsp15 complex and hydrolyze the peptidyl-tRNA ester bond without needing a stop codon-recognizing domain.

Residues 10–112 of YaeJ have a significant 29% identity and 55% similarity with the small human protein ICT1, indicating that both share the same fold. ICT1 is a 23.6-kDa protein with unknown function, but it becomes more highly expressed upon

neoplastic transformation of colon epithelial cells[19] and is predicted with high significance ($P>0.9$) to be targeted to mitochondria.[20] On the basis of its GGQ peptidyl hydrolase domain, ICT1 is classified as a putative release factor, even though, like yaeJ, it lacks an anticodon-recognizing domain. If ICT1 recycles stress-induced mitochondrial 50S•nc-tRNA complexes, this might explain its upregulation in neoplastic transformation, which is a process requiring the inhibition of apoptosis, for instance by the reduction of mitochondrial stress. Details will differ, as we did not find a eukaryotic homolog of Hsp15.

In this work, the SecM peptide was chosen for a practical reason—to stabilize the complexes by interaction of the nascent polypeptide with the ribosomal tunnel. However, this is a very unique peptide that causes translational arrest, prompting the question on whether it is valid to extrapolate the results to the general case. However, the presence of the SecM peptide is necessary, although not sufficient, for ribosome stalling: puromycin can still efficiently attack a tRNA carrying the SecM peptide,[7,21] indicating the P-site location of the tRNA moiety in the 70S complex and a functional peptidyl transfer center. Full stalling by the SecM peptide additionally requires the presence of Pro–tRNAPro at the A site.[21] In the stalled 50S subunit, this second condition cannot be met for obvious reasons, so the SecM-stalled nc-tRNA•50S complex most likely does represent the general case of a heat-shocked 50S•peptidyl-tRNA complex. In addition, the finding that Hsp15 only has specificity for 50S ribosomal subunits with a tRNA, regardless of the sequence of the nascent chain,[6] further supports the general relevance of our finding. In conclusion, we propose that Hsp15 rescues heat-induced abortive 50S•nc-tRNA subunits by fixing the tRNA moiety to the P site, regardless of the nature of the nascent chain (Fig. 1). This allows a (specialized) release factor to bind at the A site and cleave the aminoacyl ester bond between the tRNA and the nascent chain. The cleavage allows the tRNA and the nascent chain to diffuse away and the 50S particle to become translationally active again.

Experimental Procedures

Preparation of 50S·nc-tRNA complexes

The plasmid pUC19Strep3FtsQSecM was transcribed *in vitro* and translated in a membrane-free *E. coli* cell extract as previously described.[7] The translation mix was loaded directly onto a 38-ml sucrose gradient [10%–50% sucrose in 50 mM Hepes–KOH, 100 mM KOAc and 0.3 mM $Mg(OAc)_2$, pH 7.5] and centrifuged for 15 h at 23,000 rpm and 4 °C in a SW32 Ti rotor (Beckman Coulter). The 50S fraction was loaded onto a 300-μl StrepTactin Sepharose column (IBA, Göttingen, Germany) equilibrated with buffer 1 [20 mM Hepes–KOH, 150 mM NH4Cl, 1 mM $Mg(OAc)_2$ and 4 mM β-mercaptoethanol, pH 7.5] at 4 °C, eluted with 2.5 mM desthiobiotin in buffer 2 [20 mM Hepes–KOH, 150 mM NH4Cl, 12 mM Mg $(OAc)_2$ and 4 mM β-mercaptoethanol, pH 7.5] and pelleted by ultracentrifugation [3 h, 55,000 rpm, 4 °C, TLA-55 rotor (Beckman)]. The 50S•nc-tRNA (50S·nc) pellet was dissolved in buffer 2 by gentle shaking on ice.

Purification of Hsp15

The plasmid pTHZ25[1] was transformed in *E. coli* BL21 (DE3), and the cells were cultured as previously described. Cells were ruptured by two passages through an EmulsiFlex-C5 homogenizer (Avestin) at 15,000 psi, and the lysate was cleared by ultracentrifugation [1 h, 18,000 rpm, 4 °C, Ti70 rotor (Beckman)]. The supernatant was loaded onto a Q Sepharose FF column (GE Healthcare) and a phenyl-Sepharose column (GE Healthcare) as previously described.[1] The purified protein was dialyzed against 30 mM Hepes–KOH and 1 mM ethylenediaminetetraacetic acid, pH 7.0, concentrated with a Centriplus concentrator (molecular mass cutoff=3 kDa, Amicon), flash frozen and stored at −80 °C.

Binding assays of Hsp15

50S•nc, 50S and 70S (15 μg of each) were incubated in 1:1 and 1:10 molar ratios with purified Hsp15 in buffer 3 [20 mM Hepes–KOH, 100 mM NH_4Cl and 25 mM $Mg(OAc)_2$, pH 7.5] on ice for 30 min. The mix was centrifuged for 5 min at 14,000 rpm in a table-top centrifuge at 4 °C and then loaded onto a 1.5-ml sucrose cushion (30% w/v sucrose in buffer 3). The ribosomes and ribosomal subunits were pelleted by ultracentrifugation [5 h, 55,000 rpm, 4 °C, TLA-55 rotor (Beckman)]. The ribosomal pellet was quantified and loaded onto 16% SDS gel.

Puromycin assay

50S•nc-tRNA·Hsp15 complex (60 nM) in buffer 2 (or buffer 2 with increased Mg^{2+} concentration to 100 mM to favor Hsp15 dissociation) was incubated with 2 mM puromycin for 3 h at 37 °C. Samples at 45-min intervals were withdrawn, mixed with an equal volume of loading buffer and separated on low-pH SDS-based Tris–acetate gel to minimize hydrolysis of the ester bond linking tRNA to the nascent chain.[22] Immunodetection of the nascent chain was carried out on PVDF membrane using a Strep-tag monoclonal antibody conjugated to horseradish peroxidase (IBA). Detection was performed by electrochemiluminescence, and spots on the X-ray films were quantified densitometrically.

Specimen preparation and cryo-EM

For grid preparation, a 20-fold molar excess of Hsp15 was added to 150 nM 50S•nc-tRNA complexes. Glow-discharged, carbon-coated lacey Formvar grids (300 mesh, Ted Pella) were loaded with a 3-μl sample (approximately 150 nM concentration of ribosomal complex). Grids were blotted and plunged into liquid ethane using a fully automated home-built environmental chamber and vitrification device operating at 100% humidity and 25 °C. Micrographs were recorded on film at a magnification of 50,000× under low-dose conditions($<10e^{-}/Å^2$) with an FEI Tecnai F20 electron microscope operated at 200 kV using a defocus range of 1.5–4.8 μm, taking focal pair images. Images were recorded on Kodak SO-163 film and developed for 12 min in full-strength KODAK D19b developer.

Table 1. Statistics of the three-dimensional reconstructions

	50S	50S·nc-tRNA	50S·nc-tRNA·Hsp15
No. of particles picked	8681	10,731 (defocus pairs)	33,922 (defocus pairs)
Particles used in the final three-dimensional reconstruction (%)	92	84	85
Resolution(FSC = 0.5) (Å)	23	14	10
No. of micrographs	37	42	112
Defocus range (μm) (negative)	1.6–3.5	1.5–4.1	1.5–3.5

Micrographs were scanned with a scan step of 4000 dpi on a Nikon Super CoolScan 9000 scanner, corresponding to a pixel size of 1.27 Å on the object scale.

Image processing and three-dimensional reconstruction

Single particles were selected from the EM micrographs using Cyclops.[23] We also used Cyclops to create the particle sets and manage cryo-EM micrographs. We used the unique features of Cyclops to generate masks for removing the carbon layer, large ice regions, overcrowded regions and aggregates. In order to speed up the processing, we rescaled the original photos to one-fourth of the original size by averaging 2×2 boxes, which decreased the resolution to 2.54 Å/pixel. See Fig. S1 for an example of some selected particles. We used focal pair images for reconstructing the 50S•nc-tRNA•Hsp15 and 50S•nc-tRNA complexes. Each defocus pair of micrographs was aligned by refining shift, rotation and scaling parameters prior to selecting the particles. Using Cyclops, we selected particles in the far-from-focus micrographs and mapped the coordinates to the corresponding close-to-focus micrographs. Obvious noise and ice images were filtered from the model-based auto-selected images using Cyclops. Before reconstruction, we merged the large defocus and close-to-focus images.

The particle projections were limited to 128×128 pixels, covering 325×325 Å^2. Except for the reconstruction of the free 50S subunit, the defocus was corrected with the CTFIT program of EMAN.[24] For free 50S subunit, no CTF correction was applied, all the images were low-pass filtered at the first zero crossing of the CTF, and no starting model was used. The first three-dimensional model of 50S was reconstructed with the startAny program of EMAN from a set of class averages, using cross-common lines.

The reconstruction of the complex converged only slowly, because of the low signal-to-noise ratio resulting from the low-dose conditions. In order to speed convergence, we used our cryo-EM structure of the 50S subunit with a resolution of 23 Å as a starting model for the reconstruction of the two 50S•nc-tRNA complexes. Statistics of the reconstructions are given in Table 1. We examined the uniformity of the ribosomal complexes present in the sample by reanalyzing the data using supervised classification. As starting models, we used empty 50S and 50S•nc-tRNA. The vast majority (>80%) of ribosomal complexes correlated best with the 50S•nc-tRNA starting model, indicating that the sample was essentially uniform.

Fitting X-ray structures into the EM density maps/generation of an atomic model

We used the Colores subroutine of SITUS[25] to fit the high-resolution model of the 50S subunit of the 70S *E. coli* ribosome[12] into our EM density. Subsequently, we segmented the 50S model and fitted the segments into the density map using multiple rigid-body refinement. For this purpose, we used our program LOCALFIT, which is a six-dimensional searching tool in Fourier space within which the translation and rotation ranges can be limited to ensure that the relative topology of the fragments is maintained. We started with a few segments, checking intermediate results, and ultimately fitted 57 separate rigid fragments: 23S RNA was segmented into 29 fragments (based on the secondary structure), 5S RNA was segmented into 2 fragments and every ribosomal protein was treated as a single rigid body.

Difference maps were generated by subtracting the fitted density of 50S subunit from the EM maps. To fit tRNA and Hsp15 in the difference map, we first placed the tRNA and Hsp15 manually and then improved them respectively as rigid bodies with LOCALFIT. We used the atomic model of $tRNA^{Phe}$, as there is no structure known of $tRNA^{Gly}$, the tRNA present in the 50S complex. The fit of the tRNA could be slightly improved by segmenting it into two fragments. Different types of tRNA can have different angles between the anticodon and D arm and the arm containing the acceptor stem and TΨC stem.[11] Superposition of S4 and Hsp15 was performed using the program Chimera,[26] which we also used for preparing the figures.

Accession codes

The three-dimensional EM maps of the 50S•nc-tRNA•Hsp15 and 50S·nc-tRNA complexes were deposited in the European Bioinformatics Institute Macromolecular Structure Database with accession codes EMD-1456 and EMD-1455, respectively. The fitted atomic structures of 50S•nc-tRNA•Hsp15 were deposited in the Research Collaboratory for Structural Bioinformatics Protein Data Bank with IDs 3BBX (50S), 3BBV (P-site tRNA) and 3BBU (Hsp15).

Acknowledgements

This work was supported in part by Cyttron‡ and by the Swiss National Science Foundation and the National Center of Excellence in Research Structural Biology Program of the Swiss National Science Foundation (N.B.). We thank Sascha Gutmann for Hsp15 purification, Ronald Limpens for doing part of the image acquisition and Daniel Boehringer for critically reading the manuscript.

‡ http://www.cyttron.org

Supplementary Data

Supplementary data associated with this article can be found, in the online version, at doi:10.1016/j.jmb.2008.10.079

References

1. Korber, P., Zander, T., Herschlag, D. & Bardwell, J. C. A. (1999). A new heat shock protein that binds nucleic acids. *J. Biol. Chem.* **274**, 249–256.
2. Richmond, C. S., Glasner, J. D., Mau, R., Jin, H. & Blattner, F. R. (1999). Genome-wide expression profiling in *Escherichia coli* K-12. *Nucleic Acids Res.* **27**, 3821–3835.
3. Klaholz, B. P., Pape, T., Zavialov, A. V., Myasnikov, A. G., Orlova, E. V., Vestergaard, B. *et al.* (2003). Structure of the *Escherichia coli* ribosomal termination complex with release factor 2. *Nature*, **421**, 90–94.
4. Rawat, U. B. S., Zavialov, A. V., Sengupta, J., Valle, M., Grassucci, R. A., Linde, J. *et al.* (2003). A cryo-electron microscopic study of ribosome-bound termination factor RF2. *Nature*, **421**, 87–90.
5. Petry, S., Brodersen, D. E., Murphy, F. V., Dunham, C. M., Selmer, M., Tarry, M. J. *et al.* (2005). Crystal structures of the ribosome in complex with release factors RF1 and RF2 bound to a cognate stop codon. *Cell*, **123**, 1255–1266.
6. Korber, P., Stahl, J. M., Nierhaus, K. H. & Bardwell, J. C. A. (2000). Hsp 15: a ribosome-associated heat shock protein. *EMBO J.* **19**, 741–748.
7. Schaffitzel, C. & Ban, N. (2007). Generation of ribosome nascent chain complexes for structural and functional studies. *J. Struct. Biol.* **159**, 302–310.
8. Nakatogawa, H. & Ito, K. (2002). The ribosomal exit tunnel functions as a discriminating gate. *Cell*, **108**, 629–636.
9. Helgstrand, M., Mandava, C. S., Mulder, F. A. A., Liljas, A., Sanyal, S. & Akke, M. (2007). The ribosomal stalk binds to translation factors IF2, EF-Tu, EF-G and RF3 via a conserved region of the L12 C-terminal domain. *J. Mol. Biol.* **365**, 468–479.
10. Korostelev, A., Trakhanov, S., Laurberg, M. & Noller, H. F. (2006). Crystal structure of a 70S ribosome-tRNA complex reveals functional interactions and rearrangements. *Cell*, **136**, 1065–1077.
11. Moras, D., Comarmond, M. B., Fischer, J., Weiss, R., Thierry, J. C., Ebel, J. P. & Giegé, R. (1980). Crystal structure of yeast $tRNA^{Asp}$. *Nature*, **288**, 669–674.
12. Schuwirth, B. S., Borovinskaya, M. A., Hau, C. W., Zhang, W., Vila-Sanjurjo, A., Holton, J. M. & Cate, J. H. D. (2005). Structures of the bacterial ribosome at 3.5 Å resolution. *Science*, **310**, 827–834.
13. Staker, B. L., Korber, P., Bardwell, J. C. A. & Saper, M. A. (2000). Structure of Hsp15 reveals a novel RNA-binding motif. *EMBO J.* **19**, 749–757.
14. Wohlgemuth, I., Beringer, M. & Rodnina, M. V. (2006). Rapid peptide bond formation on isolated 50S ribosomal subunits. *EMBO Rep.* **7**, 699–703.
15. Noller, H. F., Hoang, L. & Fredrick, K. (2005). The 30S ribosomal P site: a function of 16S rRNA. *FEBS Lett.* **579**, 855–858.
16. Stark, H., Orlova, E. V., Rinke-Appel, J., Junke, N., Mueller, F., Rodnina, M. *et al.* (1997). Arrangement of tRNAs in pre- and posttranslocational ribosomes revealed by electron cryomicroscopy. *Cell*, **88**, 19–28.
17. Baranov, P. V., Vestergaar, B., Hamelryk, T., Gesteland, R. F., Nyborg, J. & Atkins, J. F. (2006). Diverse bacterial genomes encode an operon of two genes, one of which is an unusual class-I release factor that potentially recognizes atypical mRNA signals other than normal stop codons. *Biology Direct*, **1**, 28.
18. Connolly, L., Penas, A. D., Alba, B. M. & Gross, C. A. (1997). The response to exoplasmatic stress in *Escherichia coli* is controlled by partially overlapping pathways. *Genes Dev.* **11**, 2012–2021.
19. van Belzen, N., Dinjens, W. N. M., Eussen, B. H. J. & Bosman, F. T. (1998). Expression of differentiation-related genes in colorectal cancer: possible implications for prognosis. *Histol. Histopathol.* **13**, 1233–1242.
20. Emanuelsson, O., Nielsen, H., Brunak, S. & von Heijne, G. (2000). Predicting subcellular localization of proteins based on their N-terminal amino acid sequence. *J. Mol. Biol.* **300**, 1005–1016.
21. Muto, H., Nakatogawa, H. & Ito, K. (2006). Genetically encoded but nonpolypeptide prolyl-tRNA functions in the A site for SecM-mediated ribosomal stall. *Mol. Cell*, **22**, 545–552.
22. Kirchdoerfer, R. N., Huang, J. J., Isola, M. K. & Cavagnero, S. (2007). Fluorescence-based analysis of aminoacyl- and peptidyl-tRNA by low-pH sodium dodecyl sulfate–polyacrylamide gel electrophoresis. *Anal. Biochem.* **364**, 92–94.
23. Plaisier, J. R., Jiang, L. & Abrahams, J. P. (2007). Cyclops: new modular software suite for cryo-EM. *J. Struct. Biol.* **157**, 19–27.
24. Ludtke, S. J., Baldwin, P. R. & Chiu, W. (1999). EMAN: semiautomated software for high-resolution single-particle reconstructions. *J. Struct. Biol.* **128**, 82–97.
25. Wriggers, W., Milligan, R. A. & McCammon, J. A. (1999). Situs: a package for docking crystal structures into low-resolution maps from electron microscopy. *J. Struct. Biol.* **133**, 185–195.
26. Pettersen, E. F., Goddard, T. D., Huang, C. C., Couch, G. S., Greenblatt, D. M., Meng, E. C. & Ferrin, T. E. (2004). UCSF Chimera—a visualization system for exploratory research and analysis. *J. Comput. Chem.* **25**, 1605–1612.